Mechanical behavior of metallic strip flexible pipes during reeling operation

Xu, Yuxin; Fang, Pan; Bai, Yong

DOI
10.1016/j.marstruc.2021.102942

Publication date
2021

Document Version
Final published version

Published in
Marine Structures

Marine Structures 77 (2021) 102942

Contents lists available at ScienceDirect

Marine Structures

journal homepage: http://www.elsevier.com/locate/marstruc

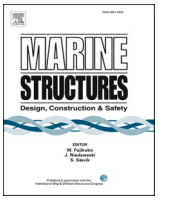

Mechanical behavior of metallic strip flexible pipes during reeling operation

Yuxin Xu [a], Pan Fang [b], Yong Bai [a,c,*]

[a] College of Civil Engineering and Architecture, Zhejiang University, 310058, Hangzhou, China
[b] Department of Maritime and Transport Technology, Delft University of Technology, 2600 AA, Delft, the Netherlands
[c] Ningbo OPR Offshore Engineering Co. Ltd, 315500, Ningbo, China

ARTICLE INFO

Keywords:
Metallic strip flexible pipe (MSFP)
Reeling operation
Experiment
Finite element simulation
Coiling drum

ABSTRACT

Metallic strip flexible pipes (MSFP), a relatively new style of unbonded flexible pipes, are considered as an attractive alternative to traditional submarine pipes. During its reeling operation, it will inevitably confront various complicated loads, which may affect the integrity and safety of MSFP's utilization. In this paper, the tension-extension and moment-curvature relation of MSFP were obtained by laboratorial tests. The mechanical properties were then imported into the global model established in ABAQUS. The finite element model was adopted to predict the deformation and mechanical responses of MSFP during the operation process. Besides, the effects of reeling length, the diameter of the coiling drum, and the pulling force were discussed. The obtained conclusions will provide some references for optimizing MSFP design and preventing possible damage in the reeling operation.

1. Introduction

Composite flexible pipes used in ocean engineering have become more and more popular due to their special properties, such as corrosion resistance and strong flexibility, which makes this type of pipes easy to transport, install and operate. As a relatively new type of composite flexible pipe, metallic strip flexible pipe (MSFP) is composed of two high density polyethylene (HDPE) layers separated by four steel strips reinforcement annular. This pipe with a sandwich structure is a particular kind of composite characterized by the combination of two different materials, contributing with their single properties to the global structure performance. Compared to other types of composite pipe, MSFP has advantages in relatively cheap reinforcement material and a simpler manufacturing process, which results in low production costs. Thus, they are regarded as a popular choice for submarine pipelines transporting oil and gas [1, 2].

During the practical manufacturing process, ready-made flexible pipelines are usually twined around a coiling drum, as shown in Fig. 1, so that much more space can be saved. It is clear that the smaller the drum's radius is, the less space it will take. Thus, more pipes can be transported at one time and the cost will be reduced. The pipes will be easier to transport because the radius of the block is normally less than 4 m, which means the reeling flexible pipes can be loaded on a truck quite conveniently, as shown in Fig. 2. However, past engineering has witnessed buckling failure concerning MFSP (Fig. 3) in reeling operation. A possible reason is that this type of pipe possesses a weak radial stiffness due to the lack of an interlocked carcass layer [3–5], plus, the loadings generated in this progress are rather complicated, inducing the pipe to buckle easily. Pipe mechanics analysis in reeling operation is illustrated in Fig. 4.

* Corresponding author. College of Civil Engineering and Architecture, Zhejiang University, 310058, Hangzhou, China.
E-mail address: baiyong@zju.edu.cn (Y. Bai).

https://doi.org/10.1016/j.marstruc.2021.102942
Received 2 June 2020; Received in revised form 30 September 2020; Accepted 16 January 2021
Available online 5 February 2021

Fig. 1. Pipe coiled in the reel drum.

Fig. 2. Pipes loaded on a truck.

Fig. 3. Buckling failure of MSFP.

Pulling force (F_T) is applied at the end of the pipeline to keep it straight. When the pipeline is fully attached to the surface of the coiling drum, the bending moment (M) reaches its peak. Meanwhile, the reaction force (q_R) is applied to the pipeline, which may result in buckling failures. To prevent possible buckling failure, there are normally three methods, namely, cross section design, constraints

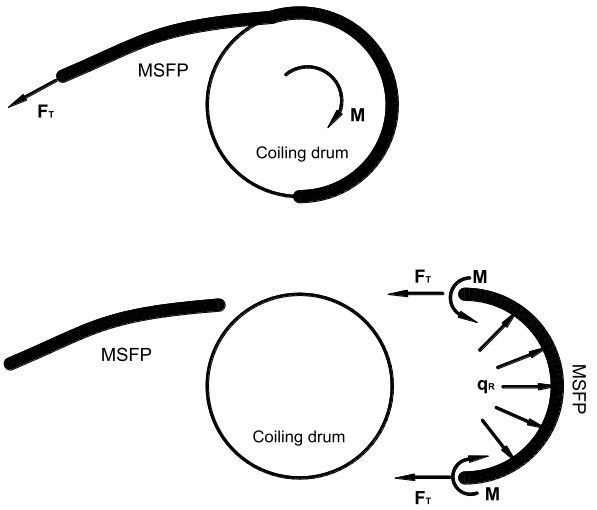

Fig. 4. Pipe mechanics analysis in reeling.

adoption and load control [6]. The maximum ovalization [7], diameter-to-thickness ratio [8,9] and length-to-diameter ratio [10] are important technical parameters to prevent buckling in cross section design. Besides, extra restriction on tubular structures may also a good way to increase the buckling capacity, such as U cross ties [11], ring-stiffeners [12] and fiber-reinforced wrap [13,14]. This paper aims to reduce the possibility of local buckling by controlling operating conditions (such as drum diameter, tension, etc.) from global aspects.

With considerable attention has been paid to the security and reliability of flexible structures in the installation and operation phases [15–19], research on their mechanical behavior during early reeling operation rarely shows in the open literature according to our review, although some similar study regarding reel-laying manipulation might provide some references. Szczotka [20] adopted the rigid finite element method to present the static and dynamic response of an offshore pipe reel-laying process. The failure phenomenon has also been observed in reel-laying manipulation. Maincon [21] pointed out that the flexible pipe may start to roll along its axis under some conditions and result in the "pig tailing" failure that makes the flexible pipe take a spiral shape. Longva & Sævik [22] proposed a new Lagrangian-Eulerian formulation for the reeling analysis, claiming that the torsion was the reason causing spiraling or various forms of damage to the tensile armor. Their following research [23] stated that torsional failures occurred to pipes transferred along a vertical-axis turn-tables placed in confined cargo holds. Four possible failure modes of pipes under severe curvature deformations and large rotations were given based on finite element simulation. The common ground in their research is that torsion is found to be the main reason for the pipe failure, which is not the same situation in reeling operation. As Ruan [24] stated that to control the resulting plastic deformation, the reasonable diameter of the reel drum was generally controlled between 15 and 25 m, which is much larger than the coiling drum in MSFP's reeling operation. Besides, the pipe's laying on the coiling drum for many cycles provokes complex combined loading, causing the pipe to fail in a different mechanism. However, current research fails to give attention to this early operation even though the failure has been identified.

To investigate how composite flexible pipes fail exactly, scholars have made a lot of effort from a local point of view [25–28]. Xu et al. [29] investigated the mechanical behavior of fiberglass reinforced bonded flexible pipe subjected to tension by experimental, theoretical and finite element method, proving that HDPE is the main component provides tension resistance during the loading process. Bahtui et al. [30] used finite element analysis software ABAQUS to simulate a flexible pipe subjected to different loads. In this model, contact elements are defined between each layer while no interaction is considered between tendons of helical armor layers. Bai and his cooperators have also completed a series of experiments, numerical and theoretical analysis about metallic pipes under various loadings, such as external pressure [31] and torsion [32]. As for combined loadings, Bai et al. [33] investigated mechanical responses of MSFP subjected to combined bending and external pressure while Dong et al. [34] proposed a model for the biaxial dynamic bending of unbonded flexible pipes. Other combined loadings on flexible pipes can also be found in the literature, such as combined bending and tension [35]. Nevertheless, considering the various loadings appearing simultaneously on flexible pipes during reeling operation, such as tension, bending, radial stress on the pipe wall etc., the study becomes much more complicated and is not fully understood. The pipeline coiled on the reeling drum is in the form of a space spiral. Besides, the friction and complex interactions between multiple layers in unbonded pipes greatly increase the difficulty of mathematical derivation and finite element analysis. The layered combination of two materials also contributes to the nonlinear behavior of MSFP. Therefore, experimental methods would be a favorable way to explore the mechanical behavior of MSFP.

The objective of this paper is to predict the global mechanical behavior of MSFP during the reeling operation before transportation. Laboratorial tests of MSFP under tension and bending were conducted to acquire its nonlinear tension-strain and moment-curvature relation. The tensile properties were introduced into the global model and the bending properties were compared with the numerical simulation results. A finite element model with MSFP, bearing plate and coiling drum was built to obtain the global mechanical responses during the reeling operation. Additional parameter analyses were done in ABAQUS to acquire the influence factors. The given

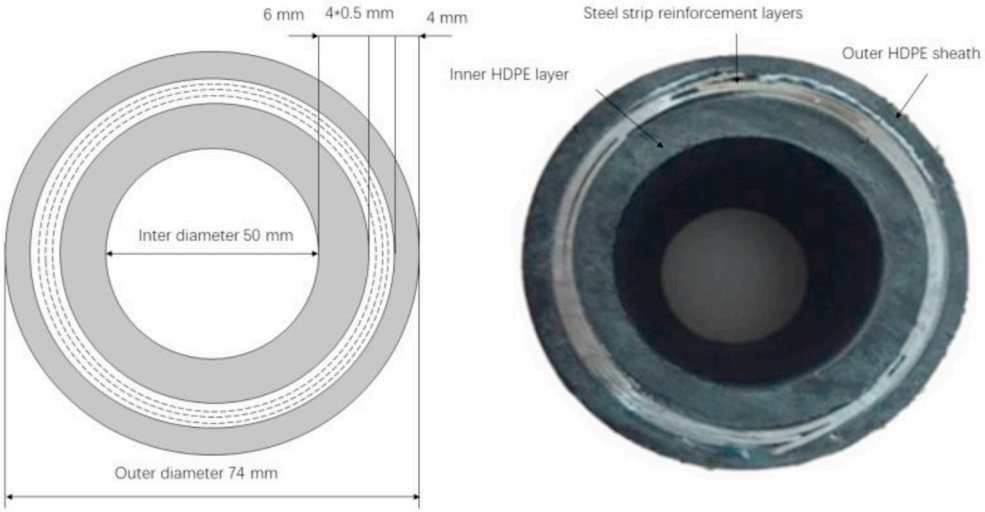

Fig. 5. Cross-section of MSFP.

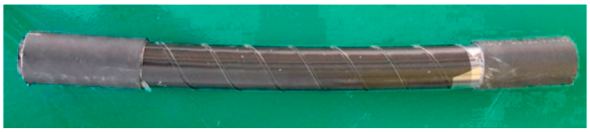

Fig. 6. MSFP with partly outer sheath peeling off.

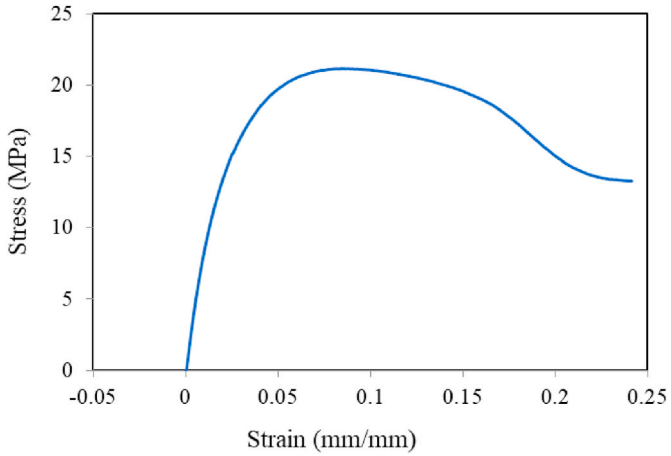

Fig. 7. Stress-strain curves of HDPE.

conclusions in this paper may provide a comprehensive concept for understanding the mechanical behavior of MSFP during reeling operation and a valuable reference for cross section design.

2. Component testing

2.1. Dimensions and material characteristics

The MSFP analyzed in this paper is produced through the helical tape wrapping method. After four reinforcement layers (two steel strips in each layer) are wound helically on the inner HDPE layer, the papery polyester tapes (PET) are then wrapped over the steel strips to prevent them from curling up, otherwise, it may lead to the piercing of the outer HDPE layer surrounded outside. The inner two reinforcement layers are wound at 54.7° in the clockwise direction with layers staggered while the other two reinforcement layers

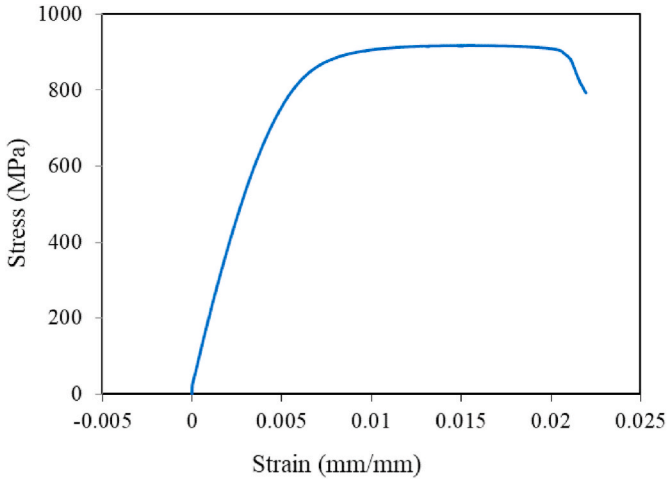

Fig. 8. Stress-strain curves of steel strip.

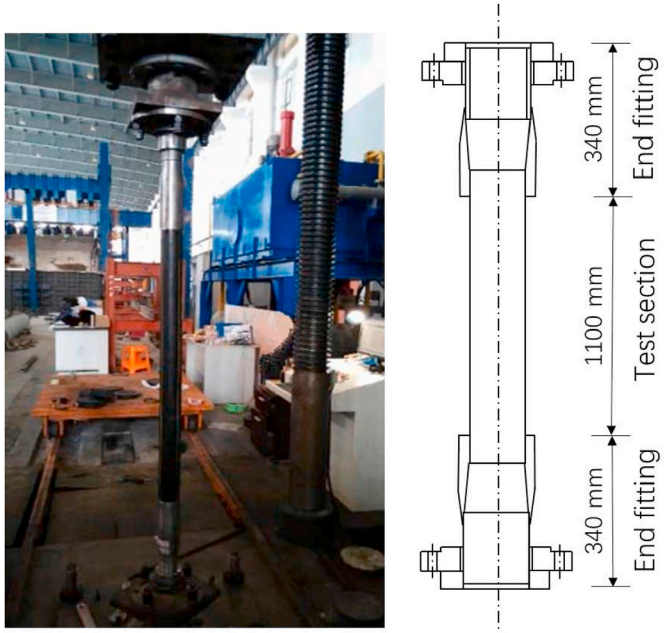

Fig. 9. Tensile test of MSFP.

are wound at 54.7° in the converse direction with layers staggered. Figs. 5 and 6 show the cross-section and the outermost reinforcement layer of MSFP. The mechanical characteristic of HDPE and steel strips used for MSFP was measured by uniaxial tensile tests and the stress-strain curves are shown in Figs. 7 and 8.

2.2. Tension test

As shown in Fig. 9, the tensile test was conducted by a 3000 kN electromagnetic servo-controlled testing machine. The specimens were connected to the machine by bolt-flange connectors to avoid the test failure caused by specimens slipping during the test. The pipe and flanges were connected by squeezing the pipe wall into the bush to form an interference fit. The space between the inner and outer sleeves was squeezed, and the serrated threads would be partially embedded in the inner and outer layers of HDPE, thereby a tight connection was formed. The axis of specimens was aligned with fixtures of the testing machine to make sure that uniform load is applied. According to (ASTM)D2105-2001 [36], the loading speed was set as 1 mm/s. The tensile tests were performed on two sets of MSFP specimens, and the corresponding tension-extension curves for two specimens are illustrated in Fig. 10.

The two curves coincide with each other relatively well, and their trend is similar to the HDPE stress-strain curve when the

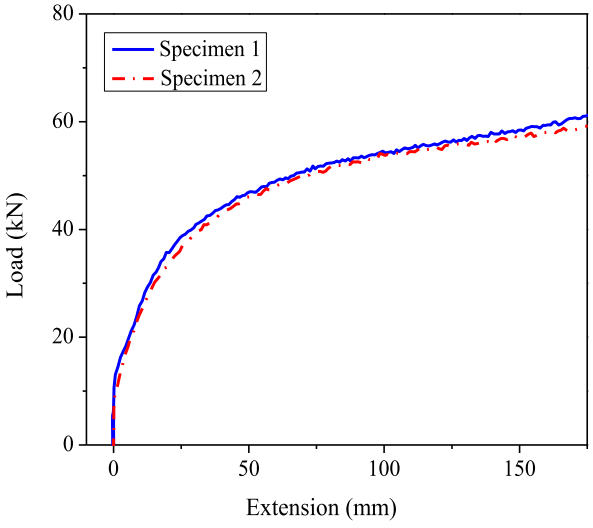

Fig. 10. Tension-extension curves of two specimens.

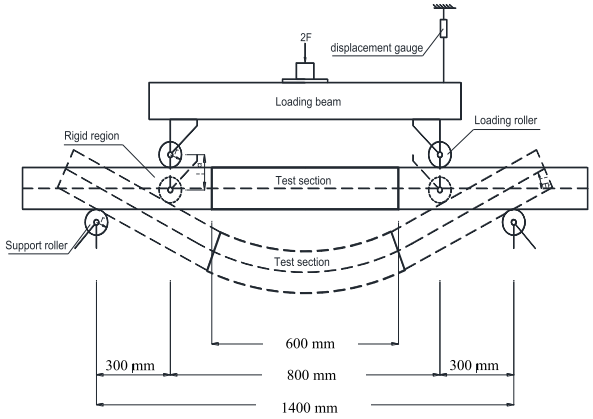

Fig. 11. Diagrammatic sketch of bending machine.

Fig. 12. MFSP specimen before and after bending.

elongation is below 10%. The yield stress of HDPE is 21 MPa, which is lower than that of the test specimens.

2.3. Bending test

Two new specimens (3 m) with free ends are used for the bending test. As shown in Fig. 11, the bending test was conducted by a

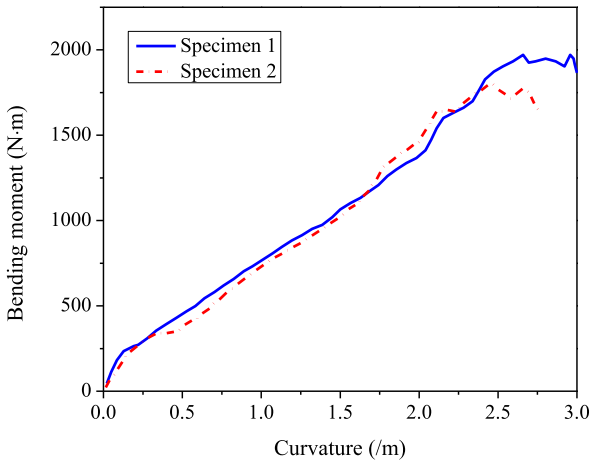

Fig. 13. Moment-curvature curves of two specimens.

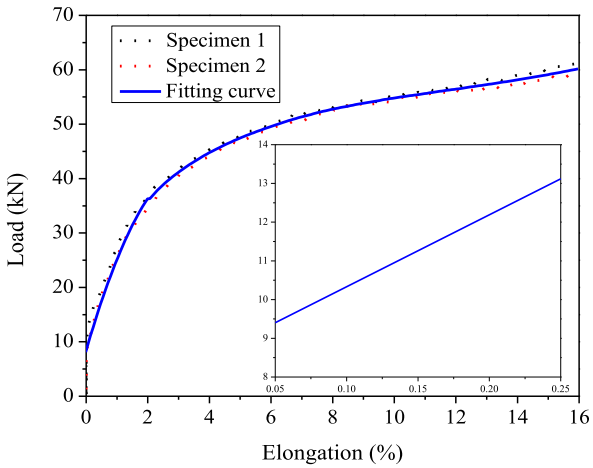

Fig. 14. Fitting tension-extension curve.

four-point bending machine. The test was carried out in the horizontal plane to eliminate the influence of the specimen's deadweight. Because the part between the support roller and loading roller is a rigid section, the test section can be considered as being subjected to pure bending. The test condition is limited by manual loading, so the loading process must be slow, stable and constant by keeping the speed of the loading beam at about 0.6 mm/s. Fig. 12 gives the deformation of MFSP specimen during the bending test. The time history of displacement and load were recorded by a displacement gauge and load sensor, respectively. The relationship between the bending moment and curvature can be deduced by data collected from the tests and geometry properties of the loading machine. The moment-curvature curves of two sets of MSFP specimens are shown in Fig. 13. The bending moment rises as the curvature increases and the two test curves are close to each other. Although the test curves have a slight fluctuation due to the man-made operation, the linear relationship between bending moment and curvature can still be observed.

2.4. Summary

In this section, tensile and bending tests of MSFP were conducted to acquire its tension-extension and moment-curvature relationship. The tension-extension relationship is input into a global model established by the finite element method and the moment-curvature relationship is used to compare with the simulation results to reveal the interaction between the combined loads. Besides, the obtained mechanical properties can also be used as a criterion for determining the failure of the pipeline in engineering applications.

Due to the uncontrollable factors during the test process, the obtained curves show certain volatility. Therefore, DataFit fitting software was employed to obtain the smooth tension-extension curve, as shown in Fig. 14. The axial stiffness is calculated as the secant modulus when the strain is 0.05% and 0.25% based on the standard ISO527-2012 [37], and the value is taken as 795.51 MPa.

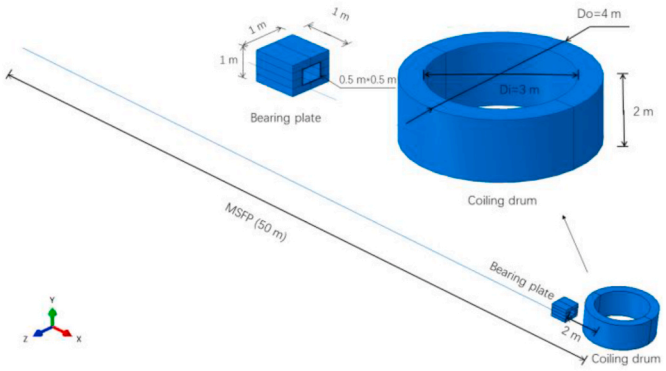

Fig. 15. The global model of reeling operation.

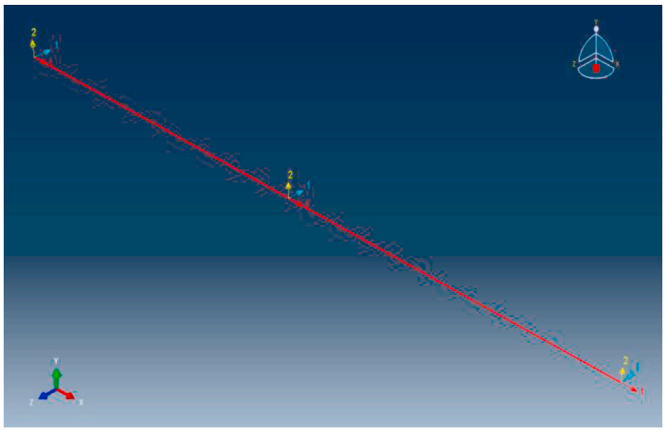

Fig. 16. The local direction of the beam element.

3. Global analysis

3.1. Modeling

The ready-made flexible pipes are usually tens of meters or even hundreds of meters, so it is impossible to simulate reeling operation without any simplification of the structure considering the limitation of computational costs. In this paper, the reeling pipeline, therefore, is simplified as a long beam owing properties akin to original MSFP in the following global analysis. The global model, shown in Fig. 15, consists of a coiling drum, a simplified pipeline, and a bearing plate. The coiling drum and bearing plate employ the discrete rigid element so that no deformation will occur in the two parts. The pipeline, however, employs deformable beam elements. Wire is used for defining the geometric shape of the pipeline to save computational costs. The fitting tension-extension relationship of MSFP obtained from Fig. 14 is then imported into the beam element cross-sectional characteristics. The local direction of the beam element is defined as shown in Fig. 16.

The diameter of the coiling drum should be no more than 4 m for conveniently transporting, as shown in Fig. 2. The coiling drum will sink slowly in the -y direction when the pipe is rolled up so that the pipe can spirally attach on the drum. The length of the pipeline is set as 50 m, which is able to wind two circles around the coiling drum. The bearing plate is employed to restrict the horizontal and vertical movement of the pipeline during the reeling operation.

3.2. Interaction and mesh

The interactions between the pipeline and the bearing plate as well as the pipeline and the coiling drum are set as surface-to-surface contact. In this scheme, because the coiling drum and bearing plate are rigid bodies, they are naturally set as master surfaces whose meshes should be coarser than those of the slave surface. The normal mechanical behavior is defined as “Hard Contact” with “Allow separation after contact”. The penalty function is taken as the tangential friction formulation. The friction coefficient between the coiling drum and the pipeline is set as 0.2 while the contact condition between the bearing plate and the pipeline is frictionless. The self-contact between twisted pipeline is not considered in this model.

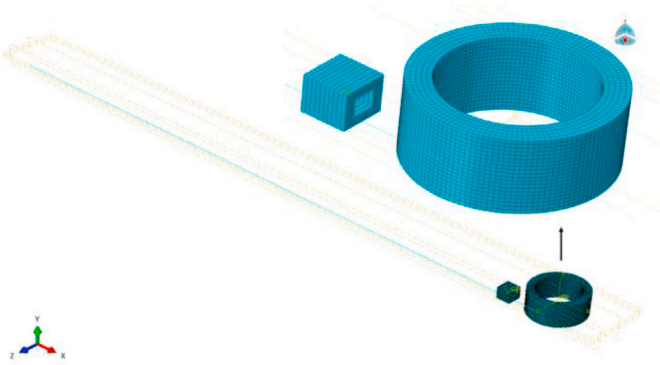

Fig. 17. Mesh condition of the global model.

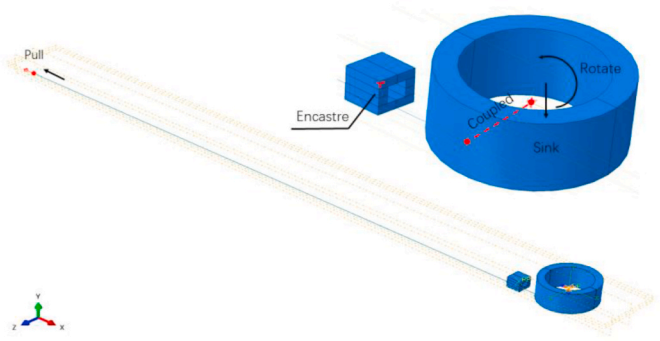

Fig. 18. Load and boundary condition of the global model.

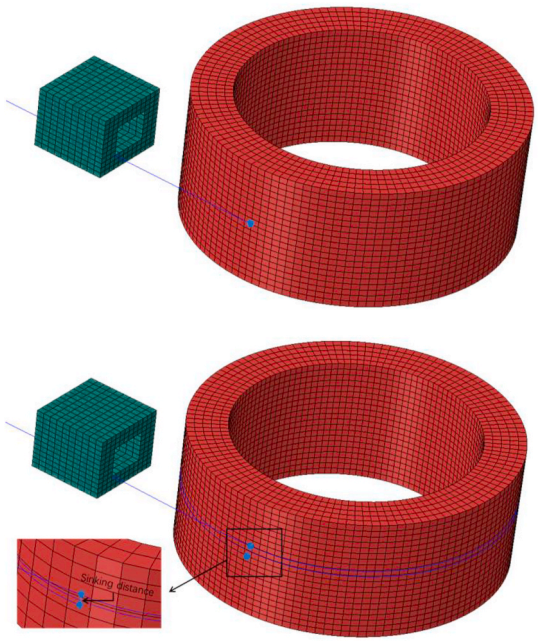

Fig. 19. The deformation of the global model.

Table 1
The definition of parameters.

Parameter	Definition
SF1 (N)	Tension
SF2 (N)	Transverse shear force in local 2-direction
SF3 (N)	Transverse shear force in local 1-2 plane
SM1 (N·m)	Bending moment around local 1-direction
SM2 (N·m)	Bending moment around local 2-direction
SM3 (N·m)	Torsion

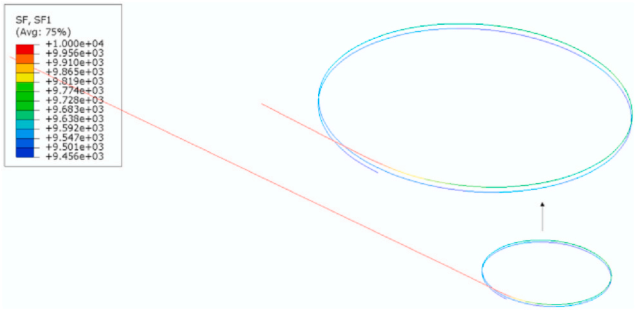

Fig. 20. SF1 of the pipeline.

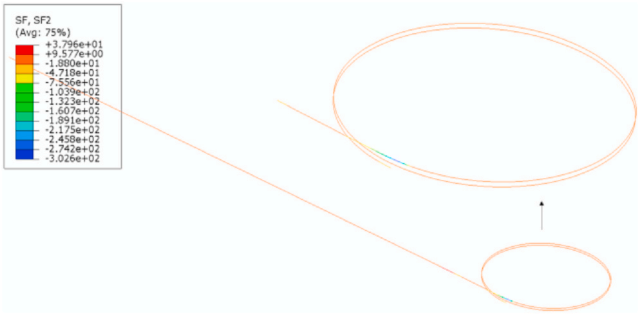

Fig. 21. SF2 of the pipeline.

A three-dimensional linear interpolation beam (B31) is selected for the pipeline because it is suitable for analyzing contact problems and also can take shear deformation into consideration. Three-dimensional beams have six degrees of freedom at each node: three translational degrees of freedom (1–3) and three rotational degrees of freedom (4–6). Furthermore, the stress components in this type of beam also provide estimates of transverse shear forces on the section. R3D3 element is used for the coiling drum and bearing plate. The mesh condition of the global model is shown in Fig. 17. The whole model contains 7736 elements. The element length used for the beam is 0.1 m.

3.3. Load and boundary conditions

The coiling drum should sink down in -y direction to make sure that the pipeline can spirally wind in an expected way. The rotation angle is 12.6 rad and the sinking distance is 0.2 m, which means the drum sinks down 0.1 m when the pipeline coils around once. Except for rotation and sinking, the displacement in the other directions is limited to 0. Thus, it means that no parts of the pipeline are overlaid on the others. In other words, no self-contact is considered in this research.

Static analysis is employed in this research, which means the coiling drum is sinking at a constant speed in one simulative step. It should be noted that there is a 10000 N pulling force applied at the end of the pipeline to keep it straight, and no other restriction on boundaries is applied. At the other end of the pipe, the start point of the pipe is coupled with the coiling drum so that they can move together. The load and boundary conditions are shown in Fig. 18.

3.4. Discussion of the results

The pipeline to be reeled keep a straight line due to the tensile force on the end and the restriction of the bearing plate when the

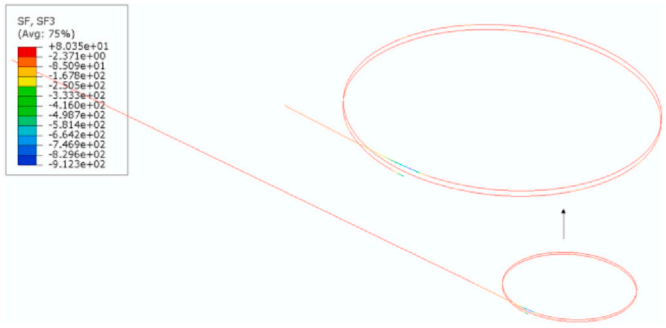

Fig. 22. SF3 of the pipeline.

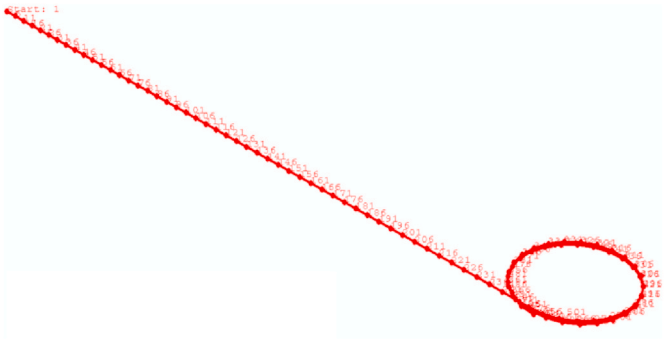

Fig. 23. A picked path for the pipeline.

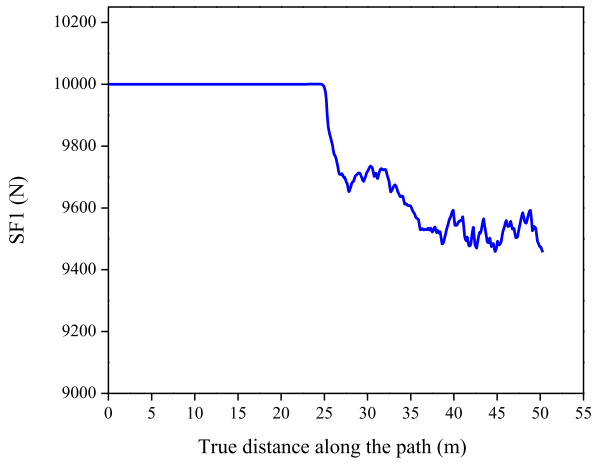

Fig. 24. SF1 along the path.

coiling drum whirls as well as sinks down. The result (Fig. 19) shows that almost two circles of MSFP adhere to the surface of the coiling drum.

Table 1 gives the definition of all parameters used in the simulative results. During the whole process, tension (SF1) along the pipeline are quite similar everywhere, almost equaling to the pulling force applied at the end. The magnitude of SF2 and SF3, however, are relatively small. Figs. 20–22 present the contour plots of forces in three directions when the reeling is finished. It can be observed that these forces are quite average in the straight section, but differ in the coiled section.

In order to obtain the stress along the pipeline after winding, a path is established along the axial direction of the pipeline, as shown in Fig. 23. The nodes are allocated on the pipe every other 0.1 m. The endpoint tension is applied at Node 1 and the endpoint adhered to the coiling drum surface is Node 501. Whereas the true distance along the path is defined from Node 1, which means the true distance at Node 1 is 0 m and the true distance at Node 501 is 50 m. Fig. 24 shows the variation of tension along the true distance. It can be

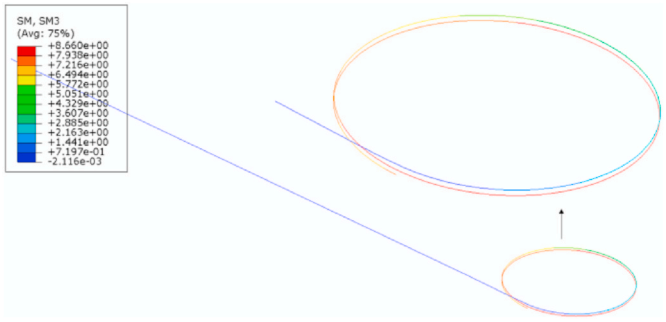

Fig. 25. Contour plot of SM3 along the path.

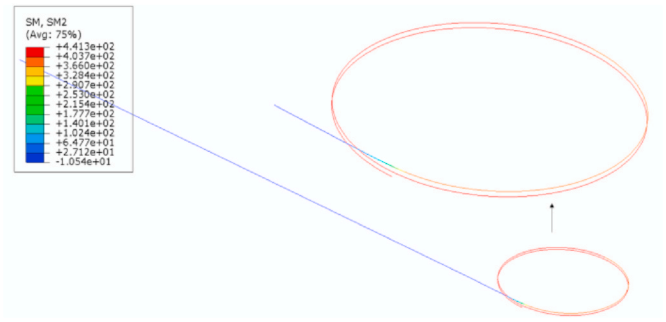

Fig. 26. Contour plot of SM2 along the path.

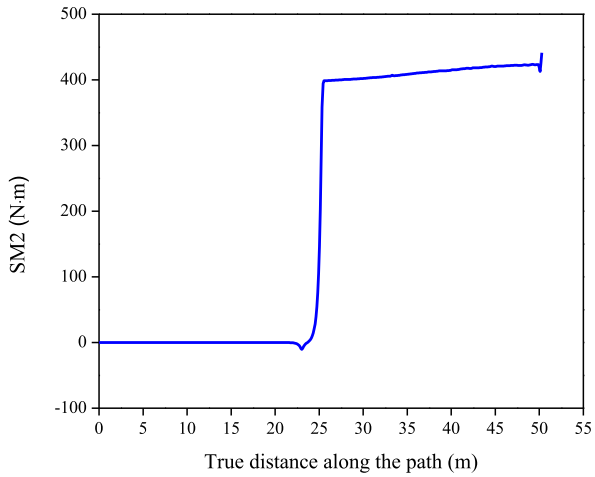

Fig. 27. SM2 along the path.

observed that SF1 has fluctuations, but the variation is quite small. The difference between the minimum value (9456.03 N) and the maximum value (10000.91 N) is 5.8%. The maximum tension shows at the distance of near 25 m (2πDo), where the pulling force begins to be affected by curvature. The pipeline stays straight before wound onto the drum and the pulling force keeps stably at 10000 N. When the pipeline starts to wind around the drum, the pulling force gradually decreases. The axial force of the pipeline coiled on the drum is smaller than the unwinding part, which means the axial force affects bending behavior to some extent.

Another load drawing more attention is the bending moment in the reeling plane, especially when the radius of the coiling drum is small. Excessive curvature resulted from the small radius would probably cause the buckling failure of the pipeline. Fig. 25 shows the twisting moment along the path. Fig. 26 shows the contour plots of bending moment (SM2) around local 2-direction when the reeling is finished, and Fig. 27 gives the relationship of corresponding bending moment and true distance along the path. It can be observed that the distribution of bending moment along the reeled pipeline is even, slightly fluctuating around 411.81 N m. Meanwhile, the unrolled pipeline does not show the existence of the bending moment. According to the MSFP bending test (Fig. 13), the corresponding bending

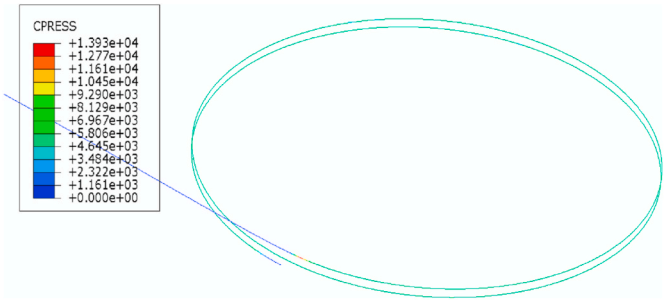

Fig. 28. Contour plot of CPRESS along the path.

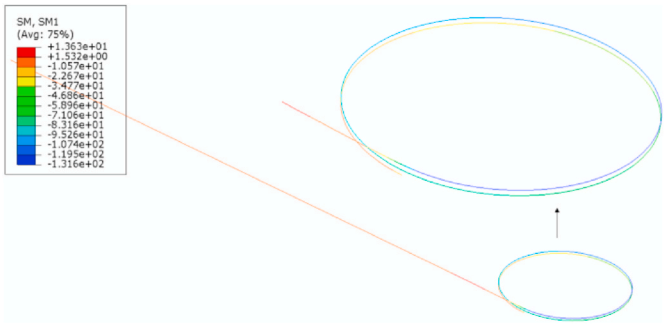

Fig. 29. Contour plot of SM1 along the path.

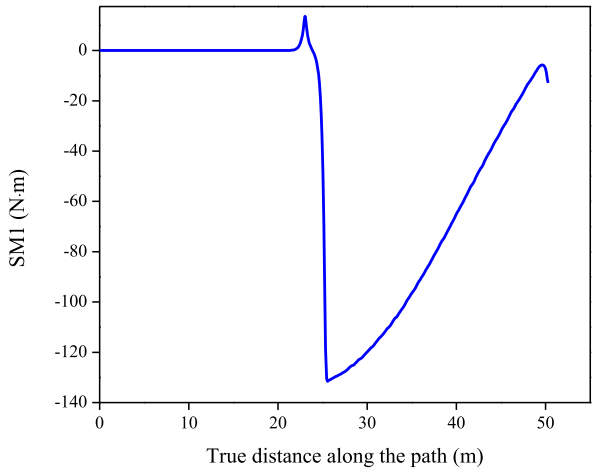

Fig. 30. SM1 along the path.

moment obtained by the curvature of the coiling drum is 452.89 N m by specimen 1 and 373.87 N m by specimen 2. The numerical magnitude is between the two experimental values with a maximum error of 10.1%. Fig. 28 gives the contour plots of contact pressure. It can be seen that the distribution of contact pressure is quite uniform, around 4.8 kPa. The maximum contact pressure (13.9 kPa) presents at the intersection of unwinding and wounded pipeline, which is much smaller than the burst pressure of MSFP (3.772 MPa) [31].

Fig. 29 presents the contour plots of SM1 distributed along the pipe when the reeling is finished. SM1 distributed along the above path is shown in Fig. 30. The bending moment SM1 of the start point of the pipeline is 0 N m and then soars at the distance of near 25 m ($2\pi Do$). The largest magnitude of the bending moment is 131.56 N m, located on the attached point between the pipeline and the bearing plate. The magnitude of SM1 then gradually decreases to 0 N m. The drum was moved downward and there is friction between the pipeline and coiling drum. The direction of the friction force is tangential to the pipe wall, which will generate a reaction force, then the reaction force acts on the pipe wall that touches the drum, inducing some torsion in the system. This could slightly change the

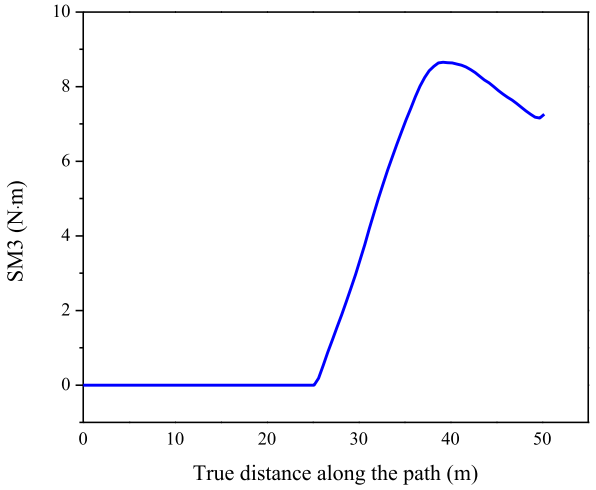

Fig. 31. SM3 along the path.

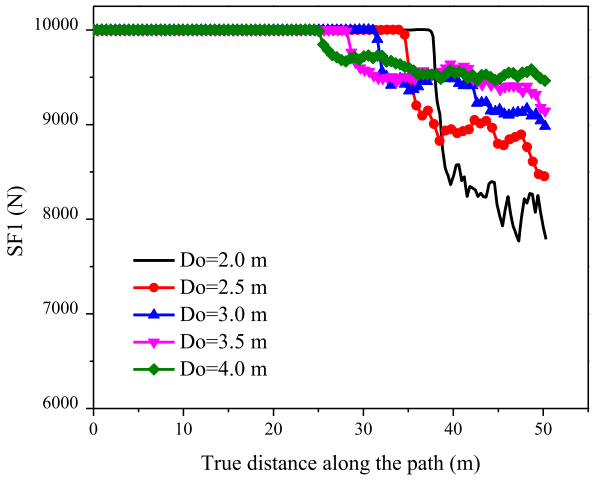

Fig. 32. SF1 along the path in different coiling drum diameter.

beam direction 1 and 2 so that SM1 is not vertical to the drum wall and SM2 is not tangential to the drum wall anymore. The maximum negative SM1 shown in Fig. 30 is close to the point where the pipeline touches the drum. The positive peak around 13.63 N m is the point lying on the bearing plate, and it presents an opposite bending moment as compared with the pipe reeling on the drum. Fig. 25 presents the distribution of SM3. Fig. 31 shows that the maximum SM3 is 8.66 N m, which is quite small compared to the bending moment in SM1 and SM2 plane. MSFP will not fail under limited single loading. However, the combination of radial compression, tensile loading and bending is very likely to be the reason for the buckling failure in the reeling operation, even the single load is much smaller than the ultimate strength.

In a word, the process of sinking the drum but keeping the encastre fixed will result in transverse forces that may induce bending moments and a tendency to twist the pipe. Therefore, engineers should pay more attention to the end of the reeled pipeline near the bearing plate in the practical reeling operation.

4. Parametric study

In this section, factors influencing the mechanical behaviors of MSFP during reeling operations are investigated by the finite element method. Other parameters should stay unchanged while only one of them is changed.

4.1. Diameter of the coiling drum

In the practical reeling process, the mechanical behavior of the pipeline can be changed by adjusting the diameter of the coiling drum, so that local buckling failure or other forms of damage can be avoided in coiling, loading and transporting. The diameter of the

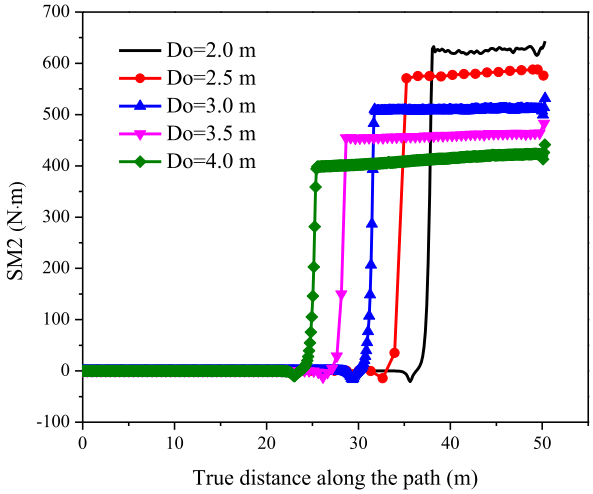

Fig. 33. SM2 along the path in different coiling drum diameter.

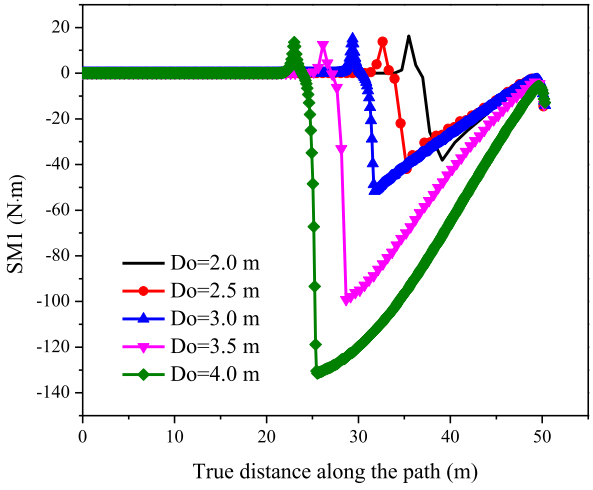

Fig. 34. SM1 along the path in different coiling drum diameter.

Table 2
The comparison of the maximum SM2 in different coiling drum diameter.

Do (m)	Numerical (N·m)	Specimen 1 (N m)	Specimen 2 (N m)
2.0	625.24	764.80	729.92
2.5	579.86	642.56	590.03
3.0	509.25	559.66	479.75
3.5	458.87	492.37	418.02
4.0	411.81	452.89	373.87

coiling drum is normally limited to 4.0 m due to convenient transportation and space limitations. Therefore, 2.0 m, 2.5 m, 3.0 m, 3.5 m and 4.0 m are selected for the coiling drum's diameter in the parameter analysis respectively.

The variables that should be paid more attention to are SF1, SM2 and SM1. The comparison results of them in each case are shown in Figs. 32–34. It can be observed that SF1 in four conditions decrease from the applied axial force of 10000 N after the pipeline attaching the bearing plate, as shown in Fig. 32. The bending moment SM2 starts from zero and then increases linearly, as shown in Fig. 33. Table 2 compares the maximum SM2 of both numerical simulation and experimental results in the same curvature. SM2 shows a downward trend as the outer diameter of the drum increases. The maximum deviation is 22.32%, and this proves the rationality of the numerical simulation method.

The bending moment SM1 increases linearly since the pipeline coiled on the drum. In addition, the larger the diameter of the coiling

Table 3
The comparison of the maximum absolute values of SM1 in different coiling drum diameter.

Do	SM1 (N·m)
2.0	38.12
2.5	41.91
3.0	51.66
3.5	99.22
4.0	131.56

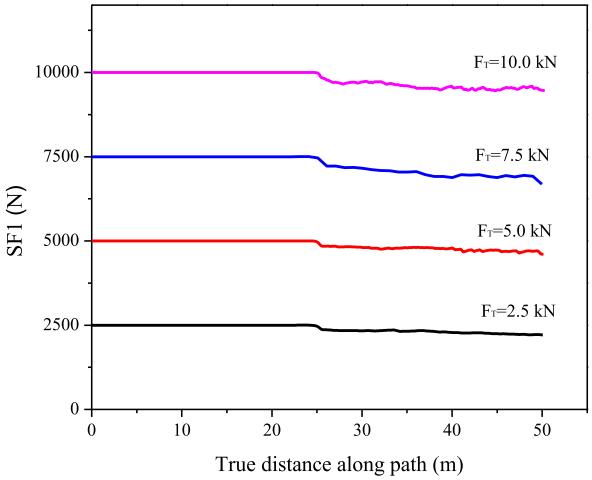

Fig. 35. SF1 along the path in different pulling force.

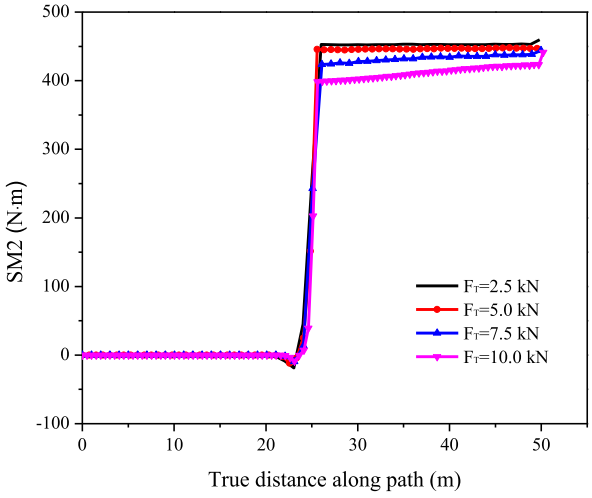

Fig. 36. SM2 along the path in different pulling force.

drum is, the bigger the maximum bending moment SM1 will achieve. The coiling loop of the pipeline is changed by the diameter of the drum, which results in the spatial spiral shape of the pipeline. Table 3 shows that SM1 is sensitive to the enlarge of drum diameter. On the other side, the torsional moment (the maximum SM3 is 8.66 N m) is quite small in all cases.

Therefore, the diameter of the coiling drum has a significant influence on the mechanical behavior of MSFP and is also the control factor of sinking speed.

4.2. Tension

In actual engineering, the deformation of the pipeline should be as small as possible before the pipeline is put into use. Fig. 10

Table 4
The comparison of the maximum SM2 in different pulling force.

F_T (kN)	Numerical (N·m)	Specimen 1 (N m)	Specimen 2 (N m)
2.5	452.83	452.89	373.87
5.0	446.31	452.89	373.87
7.5	432.86	452.89	373.87
10.0	411.81	452.89	373.87

Note: The maximum SM2 of Specimen 1 and Specimen 2 is obtained from Fig. 13 when the drum diameter is 4 m.

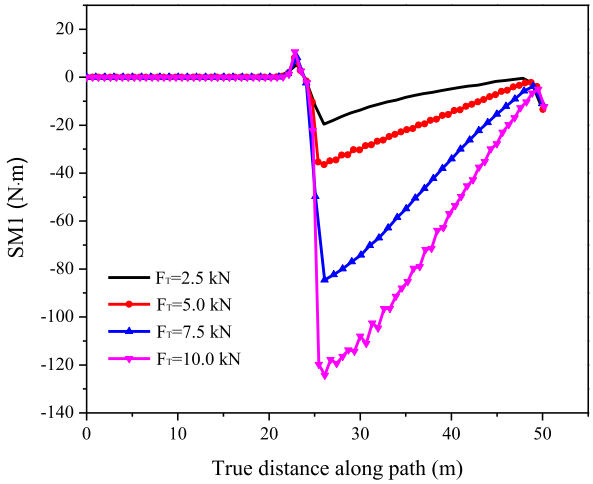

Fig. 37. SM1 along the path in different pulling force.

Table 5
The comparison of the maximum absolute values of SM1 in different pulling force.

F_T (kN)	SM1 (N·m)
2.5	19.57
5.0	36.44
7.5	84.59
10.0	131.56

indicates that the pipeline shows plastic properties when the tension is over 10.0 kN. In this analysis, tension is set as 2.5 kN, 5.0 kN, 7.5 kN, 10.0 kN. The variations of SF1 and SM2 along the path of each case are shown in Figs. 35 and 36. It can be found that the axial force SF1 changes slightly in each case. SM2 for each case has nearly the same trend before the pipeline coiling onto the drum, and then jumps to different maximum values with slight fluctuation. Table 4 compares the maximum SM2 of both numerical simulation and experimental results. The bending moment shown in Table 4 decreases with increasing tension. The effect of pulling force on the axial performance of the pipeline is decomposed to the SM2 plane, and then causes the change in SM2. Therefore, it is suggested to apply 10 kN on this kind of pipeline in the reeling process, because this value is neither too small to keep the pipe straight nor too big to induce plastic deformation.

Fig. 37 shows that bending moment SM1 in all case shares the same trend, while the maximum absolute value of SM1 increase with pulling force increasing. The maximum absolute values of SM1 in each case are shown in Table 5. This trend may be caused by the tangential contact to the pipe making the pipe bind more tightly on the surface of the drum. SM3 for each case, however, is quite small compared to the other moment. The maximum magnitude of SM3 is 8.66 N m in the above cases.

In a word, SM2 and SM1 are sensitive to the enlarge of pulling force. The magnitude pulling force should be controlled to a certain value during the reeling process to keep the pipeline straight and as less as possible plastic deformation.

4.3. Reeling length

In the actual reeling progress, the winding pipeline on the coiling drum is often multiple loops, which can ensure the integrity and uniformity of the pipeline. The winding pipeline can wind up to ten circles. In this analysis, however, the numbers of winding circles are set to 1.5, 2, 2.5 and 3.0. The variations of SF1 and SM2 along the path of each case are shown in Figs. 38 and 39.

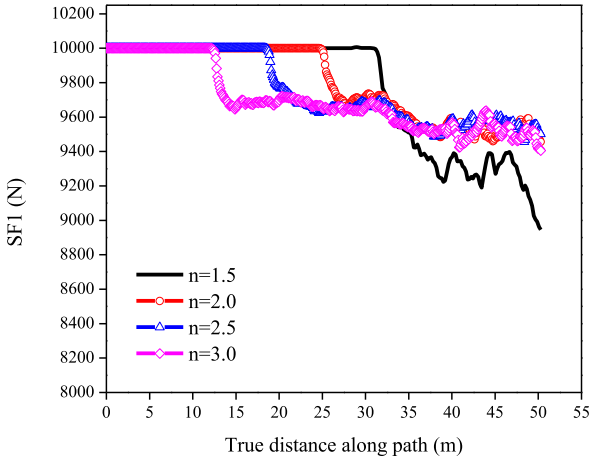

Fig. 38. SF1 along the path in different reeling length.

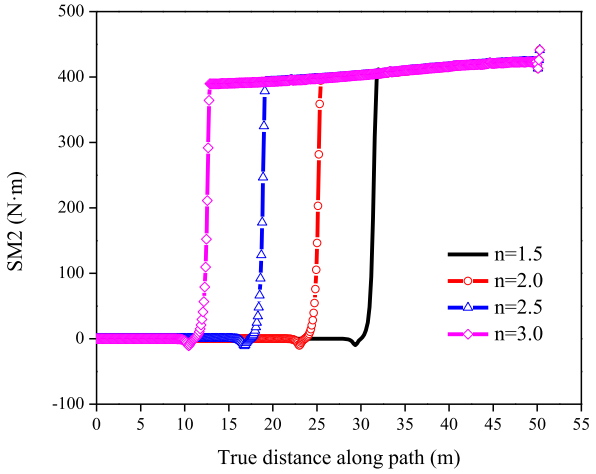

Fig. 39. SM2 along the path in different reeling length.

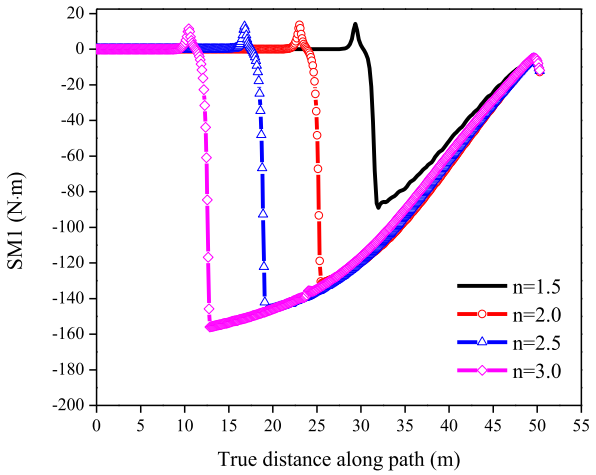

Fig. 40. SM1 along the path in different reeling length.

Table 6
The maximum SM1 in different reeling length.

n	SM1 (N·m)
1.5	89.08
2.0	131.56
2.5	147.30
3.0	155.97

It can be found that the longer the winding length of the pipeline is, the shorter the pipeline length at which the maximum axial force 10000 N is reached, and the larger the fluctuation area is. For the bending moment SM1 (Fig. 40), the longer the winding length is, the larger the maximum bending moment will be. This structure in the SM1 direction is similar to a cantilever beam. When the sinking distance is constant, the longer the cantilever beam is, the larger the bending moment is.

The section between the bearing plate and the coiling drum should be given more attention. The values of the maximum bending moment in each case are shown in Table 6. The difference between the maximum and minimum values is 75.09%, indicating that the sinking distance has a great impact on SM1. In practical reeling operation, the winding length of the pipeline can be used for controlling the maximum value of SM1. Moreover, the reeling length has no influence on the maximum bending moment SM2. This is because the outer diameters of the coiling drums and tension remain the same so that the curvatures of the reeled pipes also remain quite similar. SM3 is very small in all cases with a maximum magnitude of 8.98 N m.

5. Conclusions

In this paper, the mechanical behavior of MSFP during reeling operation is investigated by numerical and experimental methods. Tensile and bending tests were conducted to get the tension-extension and moment-curvature relation. The tension-extension relationship of MSFP was then invoked into the global analysis model in which deformation and forces were predicted and presented. After that, an extensive parametric analysis using FEM was carried out to study the influencing mechanisms on MSFP. The rationality of the simulative method was partly verified by the experimental results. Beneficial conclusions can be drawn as follows:

- The tensile force in the pipe distributes quite uniformly without too much variation, and it should be controlled to a reasonable value (10 kN) that keeps the pipe straight and reel successfully without big plastic deformation.
- Local buckling of MSFP in the reeling operation is not likely induced by torsion, which is different from current findings. The combination of radial compression, tensile loading and bending is very likely to be the reason for the buckling failure in the reeling operation, even the single load is much smaller than the ultimate strength.
- The spatial spiral shape coiled on the drum has a significant influence on the bending moment, which can be altered by the diameter of the coiling drum and the reeling length.

Declaration of competing interest

The authors declare that they have no known competing financial interests or personal relationships that could have appeared to influence the work reported in this paper.

References

[1] Guttner WC, Santos CCP, Pesce CP. A finite element method assessment of a Steel Tube Umbilical (STU) cable subjected to crushing load: comparison between two and three-dimensional approaches. Mar Struct 2017;53:52–67.
[2] Vestrum O, Kristoffersen M, Polanco-Loria MA, Ilstad H, Langseth M, Borvik T. Quasi-static and dynamic indentation of offshore pipelines with and without multi-layer polymeric coating. Mar Struct 2018;62:60–76.
[3] Østergaard NH, Lyckegaard A, Andreasen JH. On modelling of lateral buckling failure in flexible pipe tensile armour layers. Mar Struct 2012;27:64–81.
[4] Gay Neto A, Martins CdA. A comparative wet collapse buckling study for the carcass layer of flexible pipes. J Offshore Mech Arctic Eng Trans ASME 2012;134.
[5] Saevik S, Thorsen MJ. Techniques for predicting tensile armour buckling and fatigue in deep water flexible risers. In: ASME 2012 31st international conference on ocean, offshore and arctic engineering, OMAE 2012, july 1, 2012 - july 6, 2012. Rio de Janeiro, Brazil. American Society of Mechanical Engineers (ASME); 2012. p. 469–82.
[6] Cai J, He S, Jiang Z, Chen Q, Zuo Z. Experimental investigation on hysteretic behavior of thin-walled circular steel tubes under constant compression and biaxial bending. Mater Struct 2016;49(12):5285–302.
[7] Zhang ZQ, Yan YH, Yang HL. A simplified model of maximum cross-section flattening in continuous rotary straightening process of thin-walled circular steel tubes. J Mater Process Technol 2016;238:305–14.
[8] Huang B, Hong ZC. Interactive buckling of Q420 welded circular tubes under axial compression. Adv Mater Sci Eng 2020;2020(3):1–14.
[9] Chen T, Su M, Pan C, Zhang L, Wang H. Local buckling of corrugated steel plates in buried structures. Thin-Walled Struct 2019;144:106348.
[10] Ebrahimi S, Zahrai SM, Mirghaderi SR. Cyclic performance evaluation of hollow structural section (HSS) and concrete-filled tube (CFT) braces. Int J Struct Stabil Dynam 2019;19:1950140.
[11] Lee HJ, Park HG, Choi IR. Eccentric compression behavior of concrete-encased-and-filled steel tube columns with high-strength circular steel tube. Thin-Walled Struct 2019;144. 106339.1-106339.11.
[12] Shahandeh R, Showkati H. Influence of ring-stiffeners on buckling behavior of pipelines under hydrostatic pressure. J Constr Steel Res 2016;121:237–52.
[13] Wang Y, Cai G, Larbi AS, Waldmann D, Tsavdaridis KD, Ran J. Monotonic axial compressive behaviour and confinement mechanism of square CFRP-steel tube confined concrete. Eng Struct 2020;217:110802.
[14] Wei Y, Wu G, Li G. Performance of circular concrete-filled fiber-reinforced polymer-steel composite tube columns under axial compression. J. Reinforc. Plast. Compos. 2014;33(20):1911–28.

[15] Gong SF, Xu P, Bao S, Zhong WJ, He N, Yan H. Numerical modelling on dynamic behaviour of deepwater S-lay pipeline. Ocean Eng 2014;88:393–408.
[16] Wang SW, Xu XS, Lu X. Movement optimization of freely-hanging deepwater risers in reentry. Ocean Eng 2016;116:32–41.
[17] Yang SH, Ringsberg JW, Johnson E. Parametric study of the dynamic motions and mechanical characteristics of power cables for wave energy converters. J Mar Sci Technol 2018;23:10–29.
[18] Yang S-H, Ringsberg JW, Johnson E, Hu Z, Palm J. A comparison of coupled and de-coupled simulation procedures for the fatigue analysis of wave energy converter mooring lines. Ocean Eng 2016;117:332–45.
[19] Leroy J-M, Poirette Y, Dupend NB, Caleyron F. Assessing mechanical stresses in dynamic power cables for floating offshore wind farms. In: ASME 2017 36th international conference on ocean, offshore and arctic engineering, OMAE 2017, june 25, 2017 - june 30, 2017. Trondheim, Norway: American society of mechanical engineers (ASME). Ocean, Offshore and Arctic Engineering Division; 2017.
[20] Szczotka M. Dynamic analysis of an offshore pipe laying operation using the reel method. Acta Mech Sin 2011:46–57.
[21] Mainçon P. Torsion in flexible pipes, umbilicals and cables under loadout to installation vessels. ASME Int Conf Ocean 2017.
[22] Longva V, Saevik S. A Lagrangian-Eulerian formulation for reeling analysis of history-dependent multilayered beams. Comput Struct 2015;146:44–58.
[23] Longva V, Saevik S. On prediction of torque in flexible pipe reeling operations using a Lagrangian-Eulerian FE framework. Mar Struct 2016;46:229–54.
[24] Ruan W, Bai Y, Zhang T, Cao Y, Liu D. Safety assessment study of a planned offshore floating platform pipelaying test. Ships Offshore Struct 2018;13:202–13.
[25] Riahi E, Yu X, Najafi M, Sever VF. D-load strength of concrete pipes with epoxy linings. J Pipeline Syst Eng Pract 2019;10.
[26] Toh W, Bin Tan L, Jaiman RK, Tay TE, Tan VBC. A comprehensive study on composite risers: material solution, local end fitting design and global response. Mar Struct 2018;61:155–69.
[27] Betts D, Sadeghian P, Fam A. Investigation of the stress-strain constitutive behavior of +/- 55 degrees filament wound GFRP pipes in compression and tension. Compos B Eng 2019;172:243–52.
[28] Hastie JC, Kashtalyan M, Guz IA. Failure analysis of thermoplastic composite pipe (TCP) under combined pressure, tension and thermal gradient for an offshore riser application. Int J Pres Ves Pip 2019:178.
[29] Xu Y, Bai Y, Fang P, Yuan S, Liu C. Structural analysis of fibreglass reinforced bonded flexible pipe subjected to tension. Ships Offshore Struct 2019;14:777–87.
[30] Bahtui A, Bahai H, Alfano G. Numerical and analytical modeling of unbonded flexible risers. J Offshore Mech Arctic Eng Trans ASME 2009;131:021401.
[31] Bai Y, Liu T, Cheng P, Yuan S, Yao D, Tang G. Buckling stability of steel strip reinforced thermoplastic pipe subjected to external pressure. Compos Struct 2016;152:528–37.
[32] Fang P, Yuan S, Cheng P, Bai Y, Xu Y. Mechanical responses of metallic strip flexible pipes subjected to pure torsion. Appl Ocean Res 2019;86:13–27.
[33] Bai Y, Han P, Liu T, Yuan S, Tang G. Mechanical responses of metallic strip flexible pipe subjected to combined bending and external pressure. Ships Offshore Struct 2018;13:320–9.
[34] Dong LL, Tu SS, Huang Y, Dong GH, Zhang Q. A model for the biaxial dynamic bending of unbonded flexible pipes. Mar Struct 2015;43:125–37.
[35] Bai Y, Ruan WD, Cheng P, Yu BB, Xu WP. Buckling of reinforced thermoplastic pipe (RTP) under combined bending and tension. Ships Offshore Struct 2014;9:525–39.
[36] Standard Test Method for Longitudinal Tensile Properties of Fiberglass (Glass-Fiber-Reinforced Thermosetting-Resin) Pipe and Tube. Astm.
[37] ISO 527. Plastics-determination of tensile properties, 1-11.12. 2012.